Optical Side Leakage Radiometry for Distributed Characterization of Anti-Resonant Hollow-Core Fibers

Qi Liu, Yizhi Sun(*), Yulin Sheng, Haoping Deng, Shoufei Gao, Yingying Wang, and Wei Ding(*)

Institute of Photonics Technology, Jinan University, Guangzhou 510632, China, dingwei@jnu.edu.cn, sunyizhi@jnu.edu.cn

Abstract *Optical side leakage radiometric measurement is implemented on anti-resonant hollow-core fibers. The metrics of propagation loss, defect location, and phase birefringence are acquired with high precision. Polarization-dependent light leakage collected by an integrating sphere is identified. ©2023 The Author(s)*

Introduction

Recent years, the rapid progress in hollow-core optical fiber (HCF) technology has provided for a brand-new light processing platform to overcome the limitations imposed on silica optical fibers, with the virtues of broadband transmission [1], low latency [2], ultralow nonlinearity [3,4], and low thermal sensitivity [5,6]. Amongst all types of HCFs, anti-resonant type of HCFs (ARFs) with tubular cladding structures, such as conjoined-tube fibers (CTF) [7] and nested anti-resonant nodeless fibers (NANF) [8] (or double NANF [9]), are the most promising ones for ultralow loss. To further improve the performance of these ARFs, it is urgently needed to in-detail learn the light guidance in the fibers by using a distributed characterization method.

For the distributed characterization of fibers, the widely adopted approaches are based on reflectometric techniques, such as optical time domain reflectometry (OTDR) [10] and optical frequency domain reflectometry (OFDR) [11]. However, the backscattered light in ARFs is difficult to detect, because it is 3 to 4 orders of magnitude lower than that in silica fibers or in photonics bandgap HCFs. Accordingly, reflecto-metric measurement in ARFs requires a costly setup for enhanced detection sensitivity, and a certain extent of sacrifice of spatial resolution seems inevitable. Moreover, a strict requirement of ultralow back reflection at the input facet of an ARF renders all the reflectometric measurements tricky for practical implementation. An alternative method is to detect the light scattering or leakage on side [12], however, to the best of our knowledge, such research in ARFs has not been reported.

In this paper, we use the optical side leakage radiometry (OSLR) to distributed characterize our in-house-fabricated ARFs with high spatial resolutions of cm level. The result validates that the OSLR is very suited to ARF because the light leakage mainly concentrates around the fiber axis in the forward direction. Our experiments also observe a polarization-dependent light leakage phenomenon, thus enabling us to identify a trace phase birefringence in an ARF of 10^{-7} level.

Experimental Setup

The setup of our OSLR is shown in Fig. 1. The ARF under test is coiled on a bobbin with the circumference of 1 m, and is spliced to a single mode fiber (SMF) for light launch from the laser source (ID Photonics, CBDX1) at 1550 nm. In the measurement, the ARF is re-spooled to another bobbin of the same size by a rewinder. A fiber rotary joint connecting two SMF pigtails provides an unchanged coupling efficiency. When the ARF under test passes through an integrating sphere of a spatial resolution of ~5 cm (Thorlabs, 2P4/M), the light leakage will be collected and sent to a

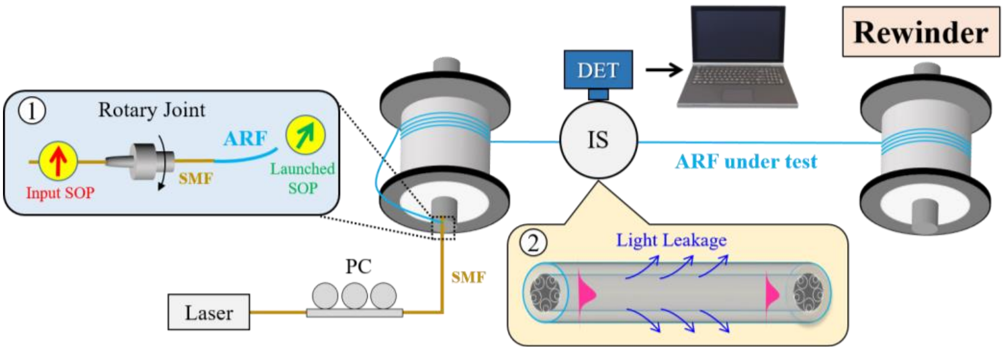

Fig. 1: The setup of the OSLR. Inset 1: variation of the launched SOP in an ARF as the fiber joint rotates. Inset 2: schematic of the side light leakage from the ARF. PC, polarization controller; IS, integrating sphere; DET, photodetector.

photodetector (Thorlabs, PDF10C/M). Then, the photocurrent is recorded in real time by a data acquisition card as a function of fiber distance.

Polarization Dependence of Light Leakage

The first sample ARF is a ~140 m long NANF (NANF#1) with a core diameter of 28 μm and an average glass wall thickness of 425 nm. The cut-back measured loss spectrum, the scanning electron microscope (SEM) image of the cross-section, and the simulated fundamental mode profiles are shown in Fig. 2(a).

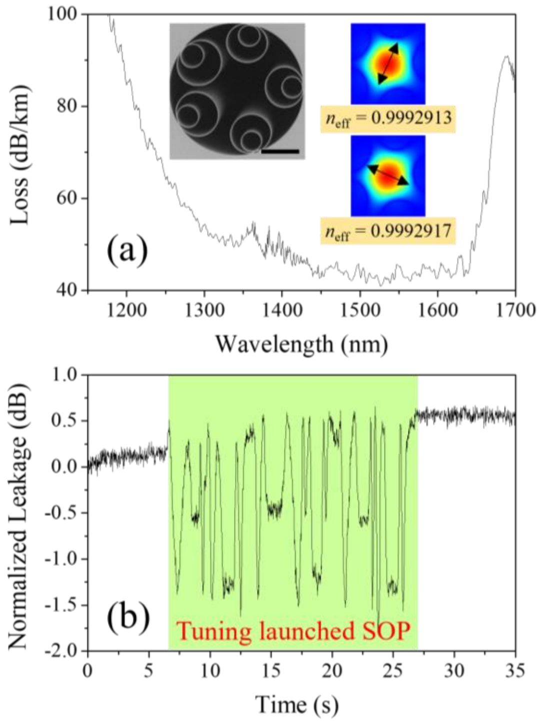

Fig. 2: (a) The cut-back measured loss spectrum of NANF#1. Inset: the SEM cross-section image and the simulated fundamental mode profiles of the two polarizations (in linear scale). Scale bar: 20 μm. (b) The measured side light leakage when tuning the SOP.

Before OSLR measurement, the polarization dependence of light leakage collected by the integrating sphere is tested. When the rewinder keeps still and the launched state of polarization (SOP) in NANF#1 is varied by tuning a 3-paddle fiber polarization controller, the intensity of the light leakage collected by the integrating sphere is recorded. As shown in Fig. 2(b), a variation of ~2 dB is manifest. Meanwhile, only a <0.2 dB variation of the transmitted light intensity is observed at the output end of the fiber rotary joint and the whole NANF#1 (after the two bobbins) when the SOP is tuned, which verifies a negligible polarization-dependent loss (PDL). The light leakage collected by the integrating sphere thus exhibits a pronounced polarization-dependent feature, probably due to the relevance of the leakage profile of an ARF with the SOP [13].

OSLR Results of NANF#1 (with high loss)

Then, the side leakage of NANF#1 is measured at a rewind speed of ~10 m/min. The original OSLR trace is shown in Fig. 3(a). A periodic fringe with a peak-to-peak value of ~2 dB appears. This can be attributed to the polarization dependence of the light leakage collected by the integrating sphere as discussed in Fig. 2(b), because the SOP in NANF#1 varies periodically as the fiber joint rotates (see inset 1 in Fig. 1). In an ARF, the coupling of the two orthogonal polarization modes can be safely ignored [14]. The red and the blue dash curves in Fig. 3(a) show the linear fits to the maxima and the minima of the fringe, giving the propagation losses of 43.1 dB/km and 43.8 dB/km, respectively, in agreement with the cut-back measured loss in Fig. 2(a).

To further study the fringe, the OSLR trace is Fourier transformed (FT) after removing the average slope, see Fig. 3(b). Several peaks appear in the FT curve. Firstly, the main peak lies at the spatial frequency of 2 m^{-1}, coinciding with the half of the circumference of our bobbin. Since the polarization in NANF#1 rotates with the period of half a circle of the bobbin, this peak (at 2 m^{-1}) obviously arises from the polarization-dependent light leakage collected by the integrating sphere. Secondly, the peak at the spatial frequency of 1 m^{-1} may come from the periodic variation of the insertion loss of our fiber

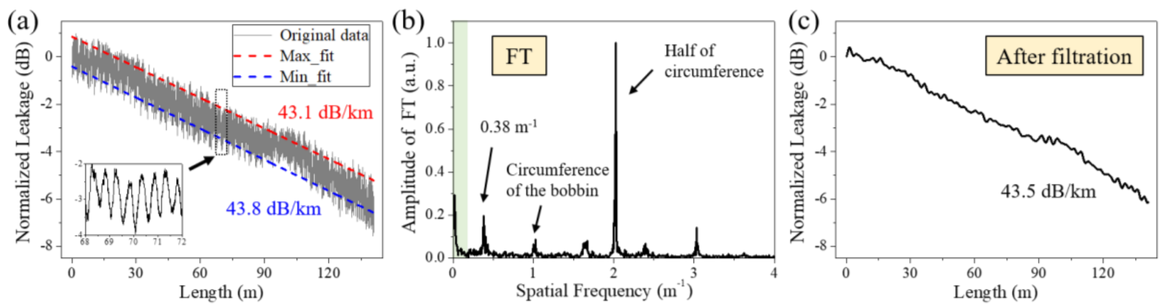

Fig. 3: (a) The OSLR measurement result of NANF#1 at 1550 nm. The inset shows a magnified view of the trace. The red and the blue dash lines are the linear fits to the maxima and the minima of the fringe, respectively. (b) The FT of the OSLR trace in (a). (c) The OSLR trace after low-pass filtration.

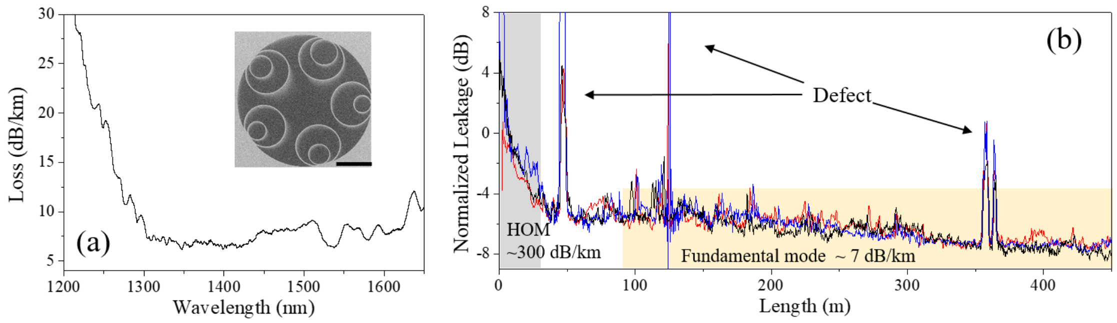

Fig. 4: (a) The measured loss spectrum of NANF#2 by cut back method. Inset: the SEM cross-section image. Scale bar: 20μm. (b) The OSLR traces of NANF#2 of three measurements after low pass filtration.

rotary joint. Thirdly, very interestingly, the peak at ~0.38 m^{-1} should be relevant to the phase birefringence of NANF#1. From the value of ~0.38 m^{-1}, the derived phase birefringence is ~5.9×10^{-7}, which is in agreement with the numerically simulated results of $\Delta n_{eff} \approx 4 \times 10^{-7}$ according to the SEM picture in Fig. 2(a). The other peaks in Fig. 3(b) appear at the sum or difference of the above three spatial frequencies.

After filtering off all the peaks outside the greenish region of Fig.3(b), Fig. 3(c) shows a smooth OSLR trace, yielding a loss of ~43.5 dB/km, which agrees very well with the cut-back measured result of ~45 dB/km.

OSLR Results of NANF#2 (with low loss)

Another 450 m long ARF sample (NANF#2) with a lower loss (~8 dB/km at 1550nm) is measured in the same way. It has a core diameter of 27 μm and an average glass wall thickness of ~450 nm. The SEM image of the cross section is shown in Fig. 4(a).

The OLSR measurement results are shown in Fig. 4(b), which have already been processed by low pass filtration. The three OSLR curves are acquired at different laser powers, coinciding well with each other. It is seen that the OLSR traces of NANF#2 can be divided into three segments---the high order mode (HOM) dominant region, the fundamental mode dominant region, and some spiky regions. In the first segment of 30 m long, the light leakage is mainly contributed by the HOM (e.g., the LP11 mode). The three curves in Fig. 4(b) show slight differences in this region, because of the different excitation conditions of HOM through a fiber splice in the three cases. An average loss of ~300 dB/km is measure in this region. After a ~50 m long transition region, the light leakage after the fiber length of 80 m mainly embodies the fundamental mode. The slope of the OSLR trace in this region is not uniform, implying the existence of a lot of microstructure defects incorporated in fabrication. The average loss of the fundamental mode is linearly fitted to be ~7 dB/km, slightly lower than the cut-back measured value of 8 dB/km. Notice that a cut-back measurement may count in more contribution from the loss of HOM, while the distributed characterization by OSLR can give many details of the tested fiber with good accuracy. Additionally, after FT of the OSLR trace, the phase birefringence of NANF#2 is measured to be ~1.86×10^{-7}, agreeing very well with the simulated result of ~1.9×10^{-7}.

Another unique merit of OSLR is precise detection of defect locations (with the spatial resolution of ~5 cm). As shown in Fig. 4(b), four peaks are clearly found at the distance of 45 m, 125 m, 357 m, and 364 m. The locations of these peaks match well in the three measurements. These peaks correspond to excessive light leakage or scattering, which are mainly caused by defects of microstructure.

Conclusions

Non-destructive and distributed characterization of ARF is realized by using OSLR method. The polarization-dependent light leakage collected by an integrating sphere is identified. This method is implemented in two in-house-fabricated NANF samples. By using Fourier analysis and spatial frequency filtration, the propagation loss, defect location, and phase birefringence of these NANFs are retrieved from the OSLR trace. This method combines high spatial resolution and potential high dynamic ranges, thus providing a unique tool to monitor the quality of ARFs.

Acknowledgements

This work was supported by National Natural Science Foundation of China (62075083, 62105122, 62222506, U21A20506); Basic and Applied Basic Research Foundation of Guangdong Province (2021A1515011646, 2021B1515020030, 2022A1515110218); Guangzhou Science and Technology Program (202201010460).

References

[1] F. Benabid, J. C. Knight, G. Antonopoulos, P. S. J. Russel, “Stimulated Raman scattering in hydrogen-filled hollow-core photonic crystal fiber”, *Science*, vol. 298, no. 5592, pp. 399-402, 2002. DOI: https://doi.org/10.1126/science.1076408

[2] F. Poletti, N. V. Wheeler, M. N. Petrovich, N. Baddela, E. N. Fokoua, J. R. Hayes, D. R. Gray, Z. Li, R. Slavik, and D. J. Richardson, “Towards high-capacity fibre-optic communications at the speed of light in vacuum”, *Nature Photonics*, vol. 7, no. 4, pp. 279-284, 2013. DOI: https://doi.org/10.1038/NPHOTON.2013.45

[3] Z. Liu, B. Karanov, L. Galdino, J. R. Hayes, D. Lavery, K. Clark, K. Shi, D. J. Elson, B. C. Thomsen, M. N. Petrovich, D. J. Richardson, F. Poletti, R. Slavík, and P. Bayvel, “Nonlinearity-Free Coherent Transmission in Hollow-Core Antiresonant Fiber”, *Journal of Lightwave Technology*, vol. 37, no. 3, pp. 909-916, 2019. DOI: https://doi.org/10.1109/JLT.2018.2883541

[4] D. Ge, S. Gao, M. Zuo, Y. Gao, Y. Wang, B. Yan, B. Ye, D. Zhang, W. Ding, H. Li, and Z. Chen, “Estimation of Kerr Nonlinearity in an Anti-resonant Hollow-Core Fiber by High-order QAM Transmission”, *Optical Fiber Communication Conference (OFC 2023)*, W4D.6, San Diego, USA, 2023. DOI: https://doi.org/10.1364/OFC.2023.W4D.6

[5] E. N. Fokoua, M. N. Petrovich, T. Bradley, F. Poletti, D. J. Richardson, and R. Slavik, “How to make the propagation time through an optical fiber fully insensitive to temperature variations”, *Optica*, vol. 4, no. 6, pp. 659-668, 2017. DOI: https://doi.org/10.1364/OPTICA.4.000659

[6] Y. Sun, Z. Liang, Y. Sheng, S. Gao, Z. Zhang, A. Jia, Y. Wang, and W. Ding, “Air flowing induced thermo-optic effect for thermal sensitivity reduction in anti-resonant hollow core fibers,” *Optics Express*, vol. 30, no. 13, pp. 23138-23148, 2022. DOI: https://doi.org/10.1364/OE.459674

[7] S. Gao, Y. Wang, W. Ding, D. Jiang, S. Gu, X. Zhang, and P. Wang, “Hollow-core conjoined-tube negative-curvature fiber with ultralow loss”, *Nature Communications*, vol. 9, no. 2828, 2018. DOI: https://doi.org/10.1038/s41467-018-05225-1

[8] F. Poletti, “Nested antiresonant nodeless hollow core fiber”, *Optics Express*, vol. 22, no. 20, pp. 23807-23828, 2014. DOI: https://doi.org/10.1364/OE.22.023807

[9] G.T. Jasion, H. Sakr, J. R. Hayes, S. R. Sandoghchi, L. Hooper, E. N. Fokoua, A. Saljoghei, H. C. Mulvad, M. Alonso, A. Taranta, T. D. Bradley, I. A. Davidson, Y. Chen, D. J. Richardson, and F. Poletti, “0.174 dB/km Hollow Core Double Nested Antiresonant Nodeless Fiber (DNANF)”, *Optical Fiber Communication Conference (OFC 2022)*, Th4C.7, San Diego, USA, 2022. DOI: https://doi.org/10.1364/OFC.2022.Th4C.7

[10] R. Slavik, E. N. Fokoua, T. D. Bradley, A. Taranta, M. Komanec, S. Zvanovec, V. Michaud-Belleau, F. Poletti, and D. J. Richardson, “Optical time domain backscattering of antiresonant hollow core fibers”, *Optics Express*, vol. 30, no. 17, pp. 31310-31321, 2022. DOI: https://doi.org/10.1364/OE.461873

[11] V. Michaud-Belleau, E. N. Fokoua, T. D. Bradley, J. R. Hayes, Y. Chen, F. Poletti, D. J. Richardson, J. Genest and R. Slavik, “Backscattering in antiresonant hollow-core fibers: over 40 dB lower than in standard optical fibers”, *Optica*, vol. 8, no. 2, pp. 216-219, 2021. DOI: https://doi.org/10.1364/OPTICA.403087

[12] S. R. Sandoghchi, M. Petrovich, D. R. Gray, Y. Chen, N. V. Wheeler, T. D. Bradley, N. H. L. Wong, G. T. Jasion, J. Hayes, E. Numkam Fokoua, M. B. Alonso, S. M. Mousavi, D. J. Richardson, and F. Poletti, “Optical side scattering radiometry for high resolution, wide dynamic range longitudinal assessment of optical fibers”, *Optics Express*, vol. 23, no. 21, pp. 27960-27974, 2015. DOI: https://doi.org/10.1364/OE.23.027960

[13] W. Ding and Y. Wang, “Semi-analytical model for hollow-core anti-resonant fibers”, *Frontiers in Physics*, vol. 3, no. 16, pp. 1-12, 2015. DOI: https://doi.org/10.3389/fphy.2015.00016

[14] A. Taranta, E. Numkam Fokoua, S. Abokhamis Mousavi, J. R. Hayes, T. D. Bradley, G. T. Jasion and F. Poletti, “Exceptional polarization purity in antiresonant hollow-core optical fibres”, *Nature Photonics*, vol. 14, no. 8, pp. 504-510, 2020. DOI: https://doi.org/10.1038/s41566-020-0633-x